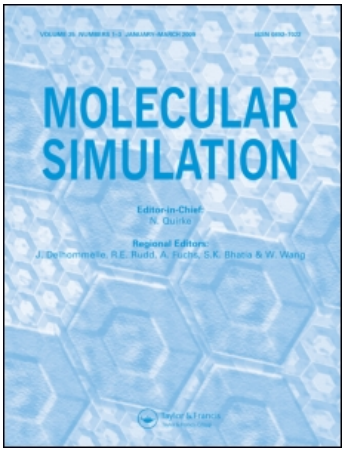

Molecular Simulation
Publication details, including instructions for authors and subscription information:
http://www.informaworld.com/smpp/title~content=t713644482

Kinetic Monte Carlo simulation for the striation distribution of void defects in Czochralski silicon growth

Sang Hun Lee[ab]; Hyun Jung Oh[a]; Do Hyun Kim[b]
[a] Simulation Part, LG Siltron, Gyeongbuk, Republic of Korea [b] Department of Chemical and Biomolecular Engineering, KAIST, Daejeon, Republic of Korea

Online publication date: 16 August 2010

To cite this Article Lee, Sang Hun , Oh, Hyun Jung and Kim, Do Hyun(2010) 'Kinetic Monte Carlo simulation for the striation distribution of void defects in Czochralski silicon growth', Molecular Simulation, 36: 9, 663 — 669
To link to this Article: DOI: 10.1080/08927021003720512
URL: http://dx.doi.org/10.1080/08927021003720512

Molecular Simulation
Vol. 36, No. 9, August 2010, 663–669

Taylor & Francis
Taylor & Francis Group

Kinetic Monte Carlo simulation for the striation distribution of void defects in Czochralski silicon growth

Sang Hun Lee[ab]*, Hyun Jung Oh[a] and Do Hyun Kim[b]

[a]*Simulation Part, LG Siltron, Imsoodong, Gumi, Gyeongbuk 730-724, Republic of Korea;* [b]*Department of Chemical and Biomolecular Engineering, KAIST, Daejeon 305-701, Republic of Korea*

(*Received 22 September 2009; final version received 22 February 2010*)

Unique crystal-originated pit (COP) distribution, similar to a striation pattern, is well matched with the oxygen profile in experimental analysis. It shows the strong relationship between oxygen concentration and COP distribution. In this paper, we study the generation of void defects and the relationship between interstitial oxygen and vacancy using the kinetic lattice Monte Carlo (KLMC) method. The KLMC method has been applied extensively in various forms to the study of micro-defects in silicon wafers. It explained well the formation of void defects such as vacancy–oxygen complex and vacancy–vacancy complex. The formation of clusters is strongly affected by oxygen concentration, which showed the relationship between COP distribution and oxygen concentration. The unique COP distribution could be correctly explained with KLMC results, and this kind of meso-scale results has not yet been reported.

Keywords: Monte Carlo method; computer simulation; defect generation; point defects; semiconducting silicon

PACS: 61.50.Ah; 61.72.Cc; 61.72.jd

1. Introduction

Crystal-originated pits (COPs) in a silicon crystal during the growth process strongly affect the gate oxide integrity characteristics of metal–oxide–semiconductor devices [1]. COPs are formed by the aggregation of excess vacancies on the primary (111) and subsidiary (100) Si planes with thin oxide films [2,3]. Many research reports on the swirl distribution of oxygen precipitates [4,5], as well as Yamagishi et al. [6] and Hasebe et al. [7] showed the striation distribution of void defects. Several researchers reported on the microscopic distribution of void defects, but the formation mechanism is not yet clarified, especially regarding the correlation of point defects and oxygen concentration.

Voronkov [8] showed that the type of grown-in defect depends on the ratio V/G (where V is the growth rate and G is the axial temperature gradient of the crystal), which defines the defect type. Many researchers reported the developing and testing of the defect simulation model. Habu and Tomiura [9] described the dominant point-defect species with a 2D continuum model. Sinno et al. [10] performed analytical calculations on the behaviour of point defects in the growing silicon crystal. The continuum models based on rate equations are most often used to make a direct comparison with experimental measurements.

Molecular dynamics (MD) calculations have been extensively used to explore the fundamental interactions between vacancies [11], and, as a result, the cluster formation energy and particle dynamics are well understood. In spite of their efficiency, MD simulation is limited to the nano-scale in both length and time scale, and in order to access a larger scale, a coarser description must be used. La Magna et al. [12] proposed a kinetic lattice Monte Carlo (KLMC) method for the description of vacancy diffusion and clustering phenomena. The KLMC method shows that the particles hop in the simulation domain according to pre-determined rates that depend on their local environment. Unlike the MD method, the KLMC method can provide valuable mesoscopic information that is difficult to obtain experimentally. Recently, Dai et al. [13] described defect formation taking into account the interaction between vacancies and oxygen. Theoretical investigation of oxygen diffusion and interaction with vacancies in silicon is difficult because of the large diffusion barrier and the complicated nature of the mixed bonding between oxygen and vacancies. Mikkelsen [14] reported an Arrhenius form, $D = 0.025 \exp(-2.53\,\mathrm{eV}/kT)$ cm^2/s, from the experimental data relating to the kinetics of oxygen diffusion.

In this paper, the formation of striation-pattern defects is well described using the KLMC model, and we present the simulation results together with the experimental results corresponding to each simulation to validate our simulations.

*Corresponding author. Email: gigantic@siltron.co.kr

ISSN 0892-7022 print/ISSN 1029-0435 online

DOI: 10.1080/08927021003720512
http://www.informaworld.com

2. Experimental analysis

Two slices of silicon wafers were cut along different crystal positions (360 and 620 mm) to observe micro-defect size and density. The micro-scale defect detection equipment MAGICS, which detects defects above 20 nm size, was used to observe the defects on wafer. Figure 1(a), (b) shows unique COP distributions on 300 mm-diameter silicon wafers taken from 360 mm-length position and 620 mm-length position of the crystal grown by the Czochralski (CZ) process, respectively. In each wafer, a ring-type COP defect distribution is present and the width of the defect distribution differs with respect to the crystal position. Secco etching confirms that there are no other defects present such as interstitial loops on the wafers. Figure 2 shows the experimental analysis results of the radial distribution of oxygen concentration in the wafers. It shows a strong relationship between COP distribution and oxygen concentration and the striation-pattern COP has originated from unbalanced oxygen concentration. The COP is usually formed by the vacancy–vacancy reaction or vacancy–oxygen reaction. These phenomena were well described by the KLMC simulation.

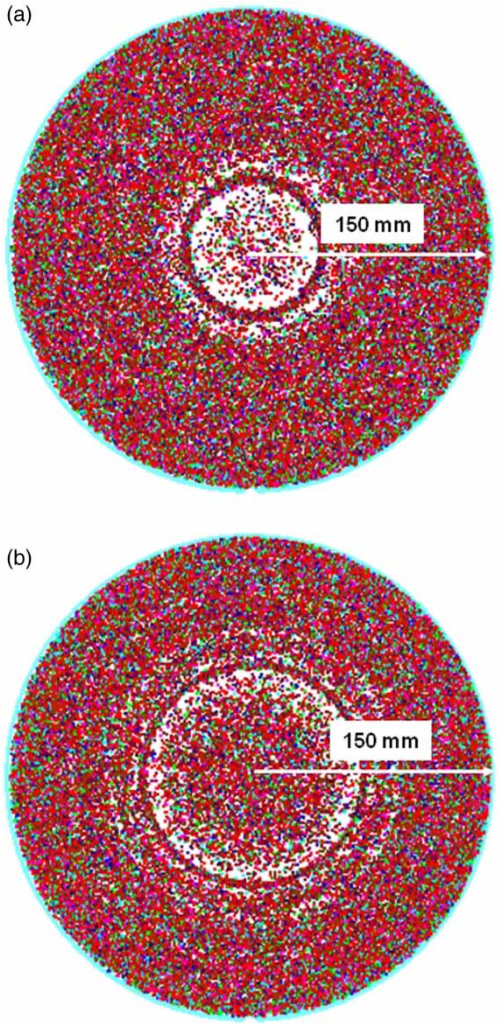

Figure 1. COP distributions of a sliced wafer: (a) 360 mm-length position of the crystal and (b) 620 mm-length position of the crystal.

3. Simulation model

3.1 Vacancy–vacancy interaction

The KLMC model has been widely used for thermal annealing and also used to describe the diffusion and clustering of vacancies in a Si lattice [15–17]. A typical move in a KLMC method consists of picking a particular event to execute, and then picking a random vacancy that can execute that event. Once the vacancy move is executed, the hopping rate of the vacancy and its surrounding neighbours is updated to reflect its new environment. As mentioned in Section 1, the principal drawback of KLMC is that mechanistic and rate information must be supplied externally. It is based on the Monte Carlo approach combined with the Poisson process [18]. The rate of a migration event is then simply given by the Arrhenius expression as follows:

$$r_i = \nu_0 \exp\left[-\frac{E_i}{k_B T}\right], \tag{1}$$

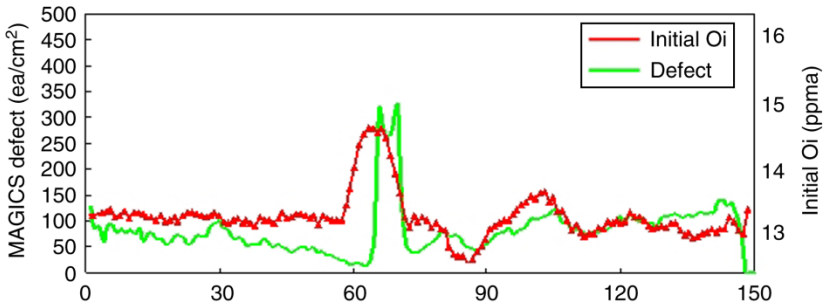

Figure 2. Radial distribution of the defect density and oxygen concentration.

where ν_0 is the attempting frequency as the prefactor and E_i is the migration energy for a single isolated vacancy, k_B is the Boltzmann constant and T is the simulation temperature; $E_i = 0.43$ eV, as reported by La Magna et al. [12], for a lattice constant of 5.43 Å. The E_i is for a single vacancy without any interaction. When a vacancy has neighbouring vacancies, E_i changes to ΔE_i, which is the energy barrier for a vacancy hop. The energy barriers for a vacancy hop are given by Dai et al. [19] as follows:

$$\Delta E_i = E_{\text{hop}} + \left(0.5 \times \sum_{j=1}^{NN} \Delta \text{NB}_j E_b^j\right), \tag{2}$$

where E_{hop} is the energy barrier for a single vacancy jump, NN is the maximum interaction shell, ΔNB_j is the change in the number of particle–particle bonds with the interaction range j and E_b^j is the corresponding binding energy.

We have implemented a lattice KMC code with the following effective atomic description of defect diffusion and clustering in Si:

(1) the defects are allowed to randomly jump to any of their four neighbouring sites and
(2) a bound state with binding energy ΔE_i forms between two defects sitting at the two nearest-neighbour sites.

Bongiorno et al. [20] investigated the formation and binding of vacancy clusters in silicon. Spherically shaped clusters are assumed in the present paper. Binding energy of nth vacancy added is defined as $E_b(n) = E_f(n-1) + E_f(1) - E_f(n)$. Table 1 shows the formation energy and the binding energy as a function of the cluster size (n). The vacancy–vacancy interaction distance is usually extended up to the second nearest-neighbour distance. In this work, the vacancy–vacancy interaction distance is extended up to the eighth nearest-neighbour shell based on previous research [21,22].

3.2 *Vacancy–oxygen interaction*

Oxygen is introduced into the crystal during solidification from the melt due to the dissolution of quartz crucible used in the CZ puller [23,24]. Single oxygen atoms exist in silicon as interstitials that occupy the puckered bond-centred sites that bridge two neighbouring silicon atoms along the $<111>$ direction [25]. There is extensive evidence for the formation of various oxygen–vacancy complexes in bulk CZ silicon, but their complexes are still under research [26]. The rate of a migration event of interstitial oxygen is several orders of magnitude slower than that of a single vacancy at all temperatures:

$$r_i = 0.0025 \exp\left[-\frac{E_i}{k_B T}\right], \tag{3}$$

where E_i is the migration energy of interstitial oxygen, k_B is the Boltzmann constant and T is the simulation temperature; $E_i = 2.43$ eV was reported by Mikkelsen [14]. Owing to the high migration energy, the diffusivity of oxygen is much smaller than that of vacancy. The formation and binding energies of the vacancy–oxygen complex in silicon [26,27] are calculated using a self-consistent total-energy pseudo-potential method. Table 2 shows the formation energy and the binding energy of the vacancy–oxygen complexes. As a consequence of strong binding, the majority of vacancies in CZ-grown Si with typical oxygen concentrations of about $10^{18}\,\text{cm}^{-3}$ are trapped by interstitial oxygen atoms, even at diffusion temperatures. The effect of vacancy trapping on the effective diffusion coefficient is defined by Casali et al. [26] as:

$$D_V^{\text{eff}} = \frac{D_V C_V}{C_V + C_{VT}}, \tag{4}$$

where C_{VT} is the concentration of trapped vacancies. As a result, the effective diffusion coefficient is strongly reduced when $C_{VT} \gg C_V$.

In this paper, we assumed that interstitial oxygen atoms and vacancies interacted in the same way as vacancies interacted with other vacancies – only the mobility of the resulting oxygen–vacancy complex was modified. Interstitial oxygen atoms in the lattice bulk are associated with compressive stresses that attract vacancies [28,29].

The time interval is set by the inverse of the net hopping rate as follows:

$$\Delta t = \frac{1}{\sum_q R_q}, \tag{5}$$

where $R_q = \sum_{i=0} r_i^q$.

Table 1. Formation energy and binding energy as a function of the cluster size (n).

Number of vacancies	E_f (eV)	E_b (eV)
1	3.4	
2	5.2	1.6
3	7.14	1.46
4	9.36	1.19
5	10.68	2.08
6	11.27	2.72
7	13.7	1.07
8	14.08	3.04

Table 2. The binding energy of vacancy–oxygen complexes.

Row	Type	Outcome	E_b (eV)
1	V + O	VO (O centre)	1.7
2	V + O	VO (O back bond)	1.2
3	V + O_2	VO_2	2.7

The time dependence of diffusivity can be expressed as a power law of the form:

$$D(t) = \sim t^{-\gamma}.$$

4. Results and discussion

Vacancy aggregation is driven by super-saturation and is responsible for the formation of void defects in silicon. The aggregation is easily influenced by temperature, vacancy–vacancy reaction and vacancy–oxygen reaction. The temperature effect is well known from previous research [30,31], and the main concern of this study is the vacancy–vacancy reaction and the vacancy–oxygen reaction. The vacancy–oxygen binding physics was not clearly defined. In our model, the oxygen–vacancy complex was formed when vacancy and interstitial oxygen meet at the nearest sites. Oxygen species did not remove the vacancy to become substitutional species and the interstitial oxygen and vacancy species stay in their sites [26,28].

Because the diffusivity of oxygen is very low, the exact nature of the vacancy–oxygen binding physics is not important for assessing the influence of bulk vacancy trapping on the evolution of vacancy–oxygen complex. The results show that the aggregate formation phenomenon is well described by vacancy cluster formation, and the generation of vacancy clusters with the oxygen–vacancy complex accounts for the striation-pattern COP defects. In this paper, the long-range interactions, which interact up to the eighth nearest neighbour, are used. The actual simulation volume was $1.6 \times 10^{-16}\,\mathrm{cm}^3$ and the total simulation time was 0.01 s.

4.1 *Vacancy–vacancy interaction*

The simulation was performed with different numbers of vacancies in a 3D simulation box with 100 unit cells in each dimension. The vacancy concentration range is from 0.5×10^{18} to $3.5 \times 10^{18}/\mathrm{cm}^2$. Figure 3 shows the diffusivity of the vacancies over time. The diffusivity decreased exponentially with $\gamma = 1.1 \pm 0.2$, where γ is the exponent, in which higher values correspond to higher concentrations. This means the clusters were formed quickly and trapped more vacancies at higher concentrations. Compared with the conditions in Haley's research [31], this paper utilises a higher system temperature and allows a wider range of vacancy concentrations, but the trend agrees well with Haley's research. Figure 4 shows the formation of the vacancy clusters over time with various vacancy concentrations. Figure 4(a) shows the number of clusters increased and then gradually decreased over time, because small clusters merged with other clusters or they were resolved into the free vacancies.

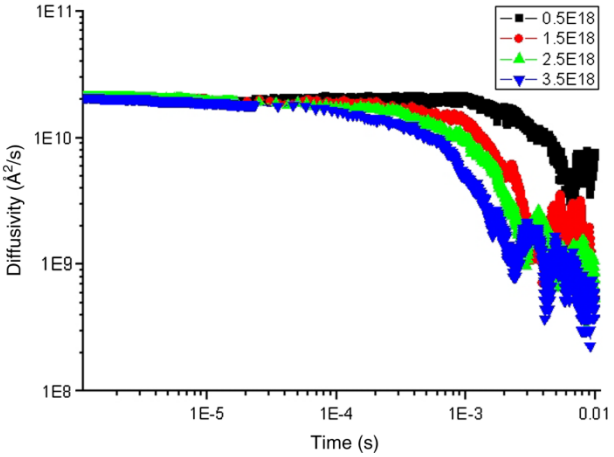

Figure 3. Diffusivity of the vacancies over time with various vacancy concentrations.

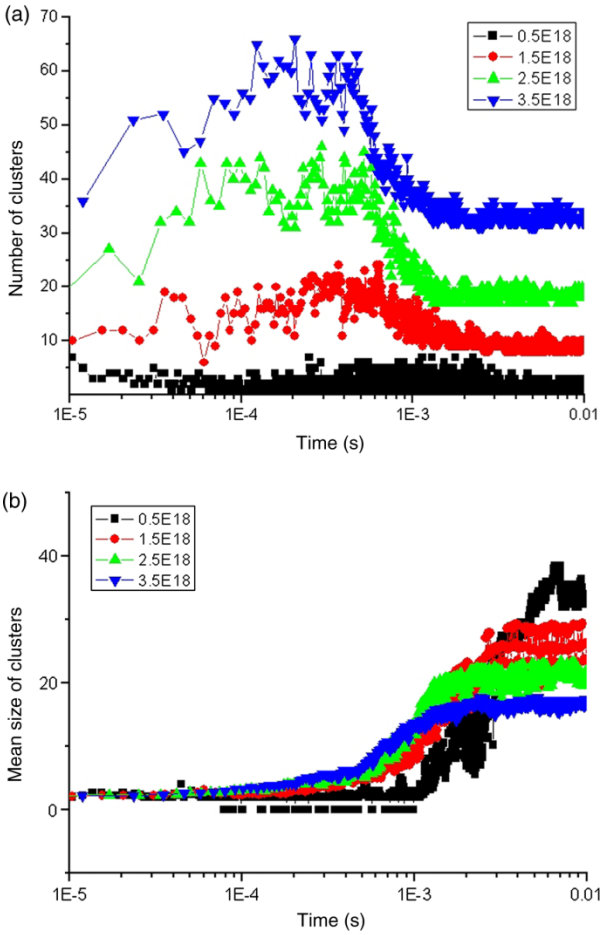

Figure 4. Formation of vacancy clusters over time with various vacancy concentrations: (a) number of clusters over time and (b) mean size of clusters over time.

The number of clusters was proportional to the vacancy concentration. Figure 4(b) shows that the mean size of the clusters increased continuously over time, but was not proportional to the vacancy concentration. Once a free vacancy was formed in a cluster, the diffusivity dramatically decreased, such that it became difficult to move and merge with neighbouring clusters. In the authors' system, the mean size of the clusters was mainly affected by the number of free vacancies. If the two systems of identical number of free vacancies existed, the system with fewer clusters will grow more than the other system with more number of clusters. Therefore, the mean size of the clusters is not proportional to the vacancy concentration. This result agrees well with the results of previous studies [31]. It implies that the defect density and size can be controlled by changing the generation of vacancy concentration.

4.2 *Vacancy–oxygen reaction*

The simulation was performed with different numbers of oxygen in a 3D simulation box with 100 unit cells in each dimension. The system temperature was 1400 K. The oxygen concentrations ranged from 0.5×10^{17} to $2.0 \times 10^{17}/\text{cm}^2$. In the case of the oxygen concentration of $2.0 \times 10^{17}/\text{cm}^2$, the number of oxygen atoms in the system is 32. In this study's model, it was assumed that the interstitial oxygen atoms moved in a manner similar to that of interstitial silicon and interacted with vacancy in the same way as vacancies interacted with other vacancies. The vacancies were easily trapped by oxygen, because the diffusivity of interstitial oxygen is several orders of magnitude lower than that of a single vacancy at all temperatures [14], and the binding energy of the vacancy–oxygen reaction is higher than that of the vacancy–vacancy reaction [27]. Figure 5 shows the diffusivity of the vacancies with increasing oxygen concentrations decreasing rapidly due to the oxygen trapping effect. The diffusivity decreases exponentially with $\gamma = 1.7 \pm 0.4$, and the exponent increased greatly when the simulation system had a higher oxygen concentration. The vacancy–oxygen reaction could have been one of the reasons for the large discrepancy between the calculated and the measured vacancy diffusion coefficients in the experiments. Figure 6 shows the formation of clusters over time with various oxygen concentrations. The cluster formation was faster than the vacancy–vacancy reaction due to higher binding energy between the vacancy and the oxygen. Figure 6(a) shows that the number of clusters increases and then gradually decreases over time, as did the vacancy–vacancy reaction. The number of clusters was proportional to the oxygen concentration. Figure 6(b) shows that the mean size of the clusters was not proportional to the oxygen concentration over time. As mentioned with respect to the vacancy–vacancy reaction, the mean

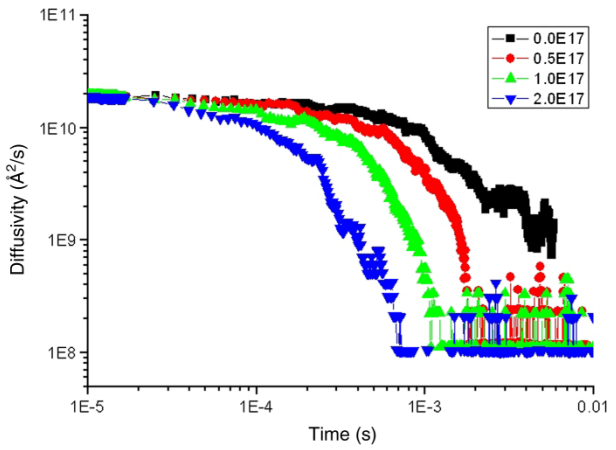

Figure 5. Diffusivity of vacancies over time with various oxygen concentrations.

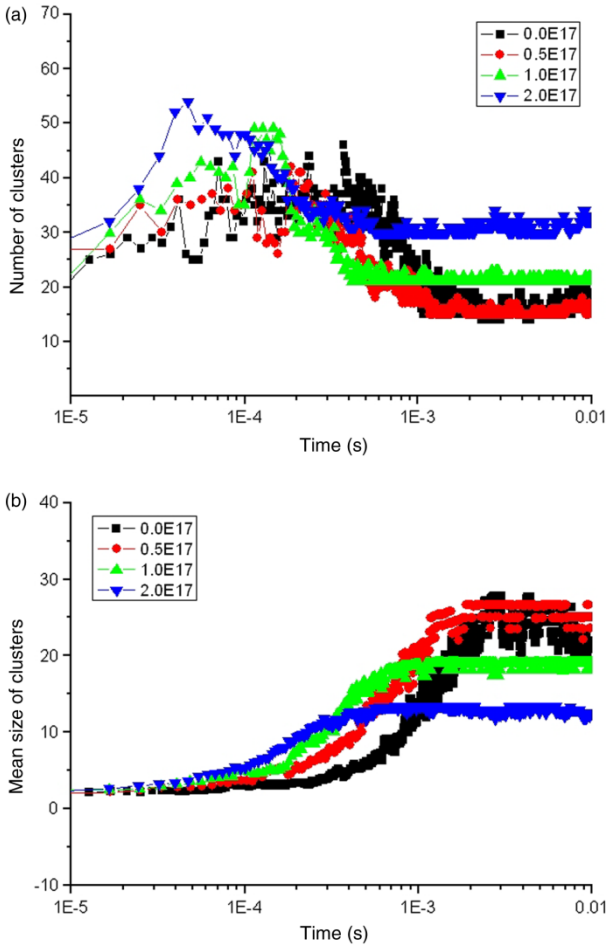

Figure 6. Formation of clusters over time with various oxygen concentrations: (a) number of clusters over time and (b) mean size of clusters over time.

cluster size was mainly affected by the number of free vacancies. Thus, the number of clusters increased with the increase in the oxygen concentration, whereas the mean cluster size decreased with the increase in the oxygen concentration. At a low oxygen concentration, the clusters that were formed had similar densities and sizes, with no influence of oxygen concentration. Figure 7 shows the formation of the clusters with various vacancy and oxygen concentrations. The oxygen concentration range was from 0 to 2×10^{17} atoms/cm^3, and the vacancy concentration range was from 0.5×10^{18} to 3.5×10^{18} atoms/cm^3. The contour plot in Figure 7(a) well explains the number of clusters according to the vacancy and oxygen concentrations. As a result, the number of clusters was proportional to the vacancy and oxygen concentrations. At lower vacancy concentrations, the number of clusters markedly increased the oxygen concentration from 0.5×10^{17} to 1.0×10^{17} atoms/cm^3, but the rate of increase of the cluster number decreased with the increase in the vacancy concentration. Figure 7(b) shows the mean cluster size according to the vacancy and oxygen concentrations. The contour plot shows that the mean cluster size increased with the decrease in the oxygen and vacancy concentrations. From these results, it is understood that cluster formation is strongly affected by the oxygen concentration. Owing to a higher binding energy, the vacancy–oxygen complex forms more easily than the vacancy–vacancy complex. If a system has a uniform vacancy concentration, the number of clusters could be dramatically increased at the locally limited high oxygen concentration area. This implies that striation-patterned void defects could have been formed in the wafer that had a unique distribution of oxygen concentrations in the experiment conducted in this study.

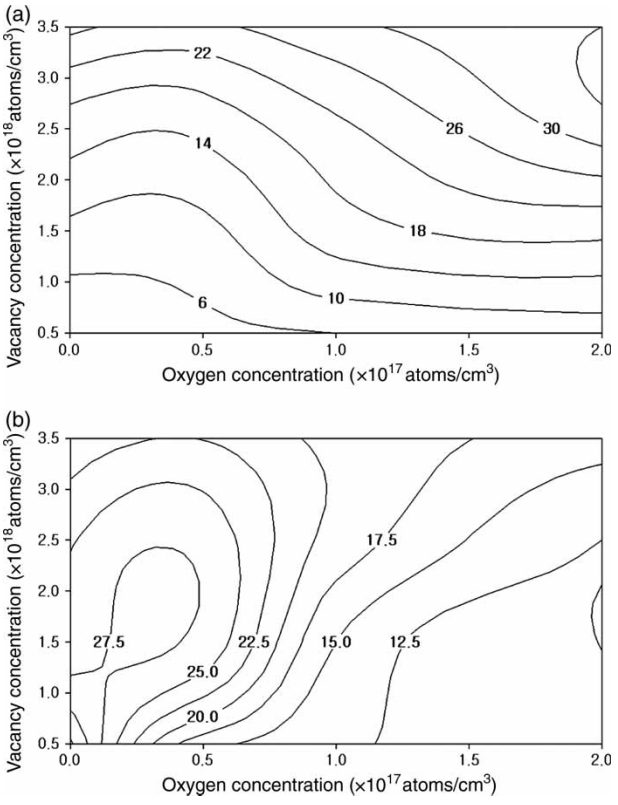

Figure 7. The formation of the clusters with various vacancy and oxygen concentrations: (a) number of clusters according to the vacancy and oxygen concentrations and (b) mean size of clusters according to the vacancy and oxygen concentrations.

5. Conclusion

In this study, vacancy cluster formation in silicon was investigated using the KLMC method, which is an effective method of estimating unique void-type defects in silicon crystal. The strong relationship between COP defects and oxygen was discovered from the experimental results. This phenomenon is well described by the KLMC method. The study results showed the vacancy clustering behaviour as a function of the vacancy–vacancy reaction and the vacancy–oxygen reaction, and the generation of defects in random order at each simulation step. The vacancy–vacancy reaction was first analysed in terms of the void formation, and showed that the number of clusters was proportional to the vacancy concentration, and the mean cluster size was not proportional to the vacancy concentration because the mean cluster size was mainly affected by the number of free vacancies. Second, the vacancy–oxygen reaction was analysed with respect to the void formation to describe the formation of striation-patterned void defects. The vacancies were easily trapped by the oxygen and thus the diffusivity of the vacancies decreased rapidly and the number of clusters increased with the oxygen concentration. The density of the clusters with the increase in the oxygen concentration agreed well with the experimental observations. When the system had a uniform vacancy concentration, the number of clusters dramatically increased at the locally limited high oxygen concentration area. Such changes in the clusters can significantly affect the dynamics of void formation. The striation-patterned COP phenomenon in the experiment was well explained, and this kind of meso-scale results has not yet been reported. These KLMC simulations can help improve the representation of such effects in macro-scale process models.

The generation of an oxygen–vacancy complex was well described by the KLMC simulation. The conditions of the KLMC simulation were given, however, by general values. With more realistic conditions for the KLMC simulation, the real experimental results could be better approximated.

Acknowledgements

We are grateful to Hyon-Jong Cho and Jang-Sub Kim for their help in obtaining excellent experimental analysis results for Figures 1 and 2.

References

[1] R. Winkler and G. Behnke, *Gate oxide quality related to bulk properties and its influence on DRAM device performance,* in *Semiconductor Silicon 1994*, H.R. Huff, W. Berghol, and K. Sumino, eds., ECS, Pennington, NJ, 1994, pp. 973–986.

[2] M. Itsumi, H. Akiya, and T. Ueki, *The composition of octahedron structures that act as an origin of defects in thermal SiO_2 on Czochralski silicon*, J. Appl. Phys. 78 (1995), pp. 5984–5987.

[3] M. Kato, T. Yoshida, Y. Ikeda, and Y. Kitagawara, *Transmission electron microscope observation of 'IR scattering defects' in as-grown Czochralski Si crystals*, Jpn. J. Appl. Phys. 35 (1996), pp. 5597–5599.

[4] J. Osaka, N. Inoue, and K. Wada, *Homogeneous nucleation of oxide precipitates in Czochralski-grown silicon*, Appl. Phys. Lett. 36 (1980), pp. 288–290.

[5] N. Inoue, J. Osaka, and K. Wada, *Oxide micro-precipitates in as-grown CZ silicon*, J. Electrochem. Soc. 129 (1982), pp. 2780–2788.

[6] H. Yamagishi, I. Fusegawa, N. Fujimaki, and M. Katayama, Proc. Symp. Advanced Science and Technology of Silicon Materials, Kona, Hawaii, Japan Society for the Promotion of Science 145th Committee, Tokyo, 1991, p. 83.

[7] M. Hasebe, J. Fukuda, T. Iwasaki, and H. Harada, *Micro-fluctuation of growth rate and grown-in defect distribution in CZ-Si*, Electrochem. Soc. Pro. 17 (2000), pp. 54–65.

[8] V.V. Voronkov, *The mechanism of swirl defects formation in silicon*, J. Crystal Growth 59 (1982), pp. 625–643.

[9] R. Habu and A. Tomiura, *Distribution of grown-in crystal defects in silicon crystals formed by point defect diffusion during melt-growth: Disappearance of the oxidation induced stacking faults-ring*, Jpn. J. Appl. Phys. 35 (1996), pp. 1–9.

[10] T. Sinno, H. Susanto, R.A. Brown, W.V. Amon, and E. Dornberger, *Boron retarded self-interstitial diffusion in Czochralski growth of silicon crystals and its role in oxidation-induced stacking-fault ring dynamics*, Appl. Phys. Lett. 75 (1999), pp. 1544–1546.

[11] A. Bongiorno and L. Colombo, *Interaction between a monovacancy and a vacancy cluster in silicon*, Phys. Rev. B 57 (1998), pp. 8767–8769.

[12] A. La Magna, S. Coffa, and L. Colombo, *A lattice kinetic Monte Carlo code for the description of vacancy diffusion and self-organization in Si*, Nucl. Instr. Meth. B 148 (1999), pp. 262–267.

[13] J. Dai, W.D. Seider, and T. Sinno, *A lattice kinetic Monte Carlo study of void morphological evolution during silicon crystal growth*, Mol. Simul. 33 (2007), pp. 733–745.

[14] J.C. Mikkelsen, Jr, *The diffusivity and solubility of oxygen in silicon*, Mat. Res. Soc. Symp. Proc. 59 (1986), pp. 19–30.

[15] L. Pelaz, L.A. Marques, M. Aboy, and J. Barbolla, *Atomistic modeling of amorphization and recrystallization in silicon*, Appl. Phys. Lett. 82 (2003), pp. 2038–2040.

[16] M. Aboy, L. Pelaz, L.A. Marques, L. Enriquez, and J. Barbolla, *Atomistic analysis of defect evolution and transient enhanced diffusion in silicon*, J. Appl. Phys. 94 (2003), pp. 1013–1018.

[17] R. Pinacho, P. Castrillo, M. Jaraiz, I. Martin-Bragado, and J. Barbolla, *Carbon in silicon: Modeling of diffusion and clustering mechanisms*, J. Appl. Phys. 92 (2002), pp. 1582–1587.

[18] K.A. Fichthorn and W.H. Weinberg, *Theoretical foundations of dynamical Monte Carlo simulations*, J. Chem. Phys. 95 (1991), pp. 1090–1096.

[19] J. Dai, J.M. Kanter, S.S. Kapur, W.D. Seider, and T. Sinno, *On-lattice kinetic Monte Carlo simulations of point defect aggregation in entropically influenced crystalline systems*, Phys. Rev. B 72 (2005), 134102.

[20] A. Bongiorno, L. Colombo, and T. Diaz De La Rubia, *Structural and binding properties of vacancy clusters in silicon*, Europhys. Lett. 43 (1998), pp. 695–700.

[21] M. Prasad and T. Sinno, *Internally consistent approach for modeling solid-state aggregation. 1. Atomistic calculations of vacancy clustering in silicon*, Phys. Rev. B 68 (2003), 045206.

[22] M. Prasad and T. Sinno, *Internally consistent approach for modeling solid-state aggregation. 2. Mean-field representation of atomistic processes*, Phys. Rev. B 68 (2003), 045207.

[23] T.A. Kinney and R.A. Brown, *Application of turbulence modeling to the integrated hydrodynamic thermal-capillary model of Czochralski crystal growth of silicon*, J. Crystal Growth 132 (1993), pp. 551–574.

[24] J.W. Corbett, R.S. McDonald, and G.D. Watkins, *The configuration and diffusion of isolated oxygen in silicon and germanium*, J. Phys. Chem. Solids 25 (1964), pp. 873–879.

[25] R.C. Jones, 1. *Early Stages of Oxygen Precipitation in Silicon*, Kluwer Academic, Dordrecht, 1996.

[26] R.A. Casali, H. Rucker, and M. Methfessel, *Interaction of vacancies with interstitial oxygen in silicon*, Appl. Phys. Lett. 78 (2001), pp. 913–915.

[27] M. Pesola, J. von Boehm, T. Mattila, and R.M. Nieminen, *Computational study of interstitial oxygen and vacancy-oxygen complexes in silicon*, Phys. Rev. B 60 (1999), pp. 11449–11463.

[28] J. Vanhellemont, *Diffusion limited oxygen precipitation in silicon: Precipitate growth kinetics and phase formation*, J. Appl. Phys. 78 (1995), pp. 4297–4299.

[29] J. Vanhellemont, *On the impact of interface energy and vacancy concentration on morphology changes and nucleation of silicon oxide precipitates in silicon*, J. Appl. Phys. Lett. 68 (1996), pp. 3413–3415.

[30] B.M. Park and I.S. Choi, *Formation behavior of grown-in defects in a vacancy-rich CZ-Si crystal*, The ECS Proceedings Series, PV 2000-17, 2000, pp. 19–21.

[31] B.P. Haley, *Vacancy clustering and diffusion in silicon: Kinetic lattice Monte Carlo simulations*, Phys. Rev. B 74 (2006), 045217.